762–774 Nucleic Acids Research, 2017, Vol. 45, No. 2 Published online 29 November 2016
doi: 10.1093/nar/gkw1130

Homologous recombination mediated by the mycobacterial AdnAB helicase without end resection by the AdnAB nucleases

Richa Gupta[1], Mihaela-Carmen Unciuleac[2], Stewart Shuman[2,*] and Michael S. Glickman[1,3,*]

[1]Immunology Program, Memorial Sloan Kettering Cancer Center, 1275 York Avenue, New York, NY 10065, USA, [2]Molecular Biology Program, Memorial Sloan Kettering Cancer Center, 1275 York Avenue, New York, NY 10065, USA and [3]Division of Infectious Diseases, Memorial Sloan Kettering Cancer Center, 1275 York Avenue, New York, NY 10065, USA

Received July 26, 2016; Revised October 26, 2016; Editorial Decision October 27, 2016; Accepted October 29, 2016

ABSTRACT

Current models of bacterial homologous recombination (HR) posit that extensive resection of a DNA double-strand break (DSB) by a multisubunit helicase–nuclease machine (e.g. RecBCD, AddAB or AdnAB) generates the requisite 3′ single-strand DNA substrate for RecA-mediated strand invasion. AdnAB, the helicase–nuclease implicated in mycobacterial HR, consists of two subunits, AdnA and AdnB, each composed of an N-terminal ATPase domain and a C-terminal nuclease domain. DSB unwinding by AdnAB *in vitro* is stringently dependent on the ATPase activity of the 'lead' AdnB motor translocating on the 3′ ssDNA strand, but not on the putative 'lagging' AdnA ATPase. Here, we queried genetically which activities of AdnAB are pertinent to its role in HR and DNA damage repair *in vivo* by inactivating each of the four catalytic domains. Complete nuclease-dead AdnAB enzyme can sustain recombination *in vivo*, as long as its AdnB motor is intact and RecO and RecR are available. We conclude that AdnAB's processive DSB unwinding activity suffices for AdnAB function in HR. Albeit not excluding the agency of a backup nuclease, our findings suggest that mycobacterial HR can proceed via DSB unwinding and protein capture of the displaced 3′-OH single strand, without a need for extensive end-resection.

INTRODUCTION

The repair of double-strand breaks (DSBs) in bacterial chromosomes is essential for bacteria to thrive and, in some cases, for bacterial pathogenesis. Mycobacteria accomplish DSB repair by deploying three distinct mechanisms: RecA-dependent homologous recombination (HR), RecA-independent single-strand annealing (SSA) and Ku/LigD-dependent non-homologous end joining (NHEJ) (1,2). Among these repair pathway options, only HR ensures faithful repair of the damaged chromosome without mutation at the DSB site. By contrast, SSA and NHEJ are mutagenic, producing either large deletions (SSA) or insertions and deletions (NHEJ). Repair by HR predominates over NHEJ and SSA in *Mycobacterium smegmatis* when a single chromosomal DSB is inflicted by the homing endonuclease I-SceI (2).

DNA recombination is a complex multi-step pathway. In the canonical model of bacterial HR, the first step is resection of the DSB by a multisubunit helicase–nuclease (3,4) to generate a 3′ tailed single-stranded DNA (ssDNA) that is initially bound by SSB. In *Escherichia coli*, this resection is initiated by the heterotrimeric RecBCD enzyme, whereas in *Bacillus subtilis* this function is performed by the heterodimeric AddAB enzyme (4,5). The next step in bacterial HR entails polymerization of RecA on the 3′ single-stranded DNA tail to form a RecA nucleoprotein filament responsible for the homology search and strand invasion into the homologous sister chromatid. Subsequent steps include DNA synthesis primed by a 3′-OH end of the invading DNA, formation and resolution of Holliday junction recombination intermediates, and residual gap filling and nick ligation to complete faithful repair. Consistent with the initiating functions of helicase–nucleases in HR, *E. coli recBCD* and *B. subtilis addAB* null mutants are clastogen-sensitive and defective for repair of DSBs (6,7).

Mycobacteria encode two helicase–nucleases: RecBCD and AdnAB (ATP-dependent nuclease AB). In sharp contrast to some well studied bacteria wherein RecBCD functions as the primary presynaptic nuclease and RecA-loader during recombination, mycobacterial RecBCD does not participate in HR (or NHEJ) and its deletion causes no

*To whom correspondence should be addressed. Tel: +1 646 888 2368; Fax: +1 646 422 0492; Email: glickmam@mskcc.org
Correspondence may also be addressed to Stewart Shuman. Email: s-shuman@ski.mskcc.org
Present address: Richa Gupta, Department of Natural Sciences, LaGuardia Community College, 31-10 Thomson Ave., Long Island City, NY 11101, USA.

significant effect on survival upon treatment with DNA clastogens or in repair of homing endonuclease-induced DSBs (1,2,8). Instead, mycobacterial RecBCD is an essential agent of the SSA pathway of DSB repair (2,9,10).

AdnAB is the helicase–nuclease implicated in mycobacterial HR, insofar as deletion of the *adnAB* operon in *M. smegmatis* elicits a ∼50% reduction in repair of I-SceI induced DSBs and hyper-sensitivity to alkylating agents, DNA cross-linkers, and ionizing radiation (IR) (2). The residual HR evident in an *M. smegmatis* Δ*adnAB* strain is mediated by the RecFOR pathway (9,11). Even in the absence of both AdnAB and RecBCD, residual RecFOR-dependent HR is maintained, suggesting that unknown helicases and/or nucleases can work in concert with the mycobacterial RecFOR machinery (2).

The AdnA (1045-aa) and AdnB (1095-aa) subunits of the AdnAB heterodimer are each composed of an N-terminal UvrD-like superfamily I helicase motor domain and a C-terminal RecB-like nuclease domain. Initial biochemical studies of the DNA-dependent ATPase (K_m 87 μM ATP; k_{cat} 415 s^{-1}), ssDNA translocase, dsDNA and ssDNA nuclease, and DSB resection activities of purified AdnAB, together with analyses of the effects of nuclease-inactivating and ATPase-inactivating mutations and 5′ and 3′ terminal obstacles on these activities (12–14), prompted a model of AdnAB end-processing shown Figure 1A, which highlights the division of labor among the two subunits and their component motor and nuclease domains. In brief, the ATP-independent binding of AdnAB to a DSB end (either blunt-ended or with short 5′ or 3′ overhangs) initiates ATP-dependent translocation of the two tandem motor domains in the 3′ to 5′ direction along the same DNA strand, with the 'leading' AdnB motor domain in the vanguard. Unwinding of the DNA duplex by the advancing motor results in pumping of the 3′ ssDNA strand into the AdnB nuclease domain and threading of the 5′ ssDNA strand through the AdnA nuclease domain. DNA translocation is stringently dependent on the ATPase activity of the lead AdnB motor, but not of the lagging AdnA motor. The posited AdnAB domain dispositions on the DNA strands during unwinding is in agreement with the crystal structure of *Bacillus* AddAB engaged on a Y-forked DNA substrate (15–17). Notable distinctions between the mycobacterial AdnAB and *Bacillus* AddAB systems are that: (i) the equivalent of the lagging motor domain in the *Bacillus* enzyme binds ATP but is not catalytically active for ATP hydrolysis; and (ii) whereas the *Bacillus* motor-nuclease is responsive to a Chi sequence that modulates its nuclease activities and triggers a recombination-promoting conformational change (18), there is no information as to whether an analogous Chi phenomenon exists for mycobacterial AdnAB.

Including mycobacterial SSB in reactions containing long linear plasmid dsDNAs enabled the study of AdnAB helicase function under conditions in which the unwound single strands are coated by SSB and thereby prevented from reannealing (or promoting ongoing ATP hydrolysis). This system, depicted in Figure 1B, models the initial end-processing phase of HR. (Note that mycobacterial SSB has been imputed to have a direct role in the subsequent formation of a RecA-bound recombination substrate (19)). We found that the AdnAB helicase motor (in which both nucleases were inactivated) catalyzed processive unwinding of dsDNAs at a rate of ∼250–270 bp s^{-1}, while hydrolyzing ∼5 ATPs/bp unwound. Crippling the AdnA phosphohydrolase active site did not affect the rate of unwinding, but lowered energy consumption slightly, to ∼4.2 ATPs per bp unwound. Mutation of the AdnB phosphohydrolase abolished duplex unwinding, consistent with the model (Figure 1A) in which the lead AdnB motor propagates the Y-fork. By tracking the resection of the 5′ and 3′ strands at the DSB ends, we verified the division of nuclease labor during dsDNA unwinding, whereby the AdnA nuclease processes the unwound 5′ strand while the AdnB nuclease incises the 3′ strand on which the motor translocates. In the presence of SSB, the AdnB nuclease makes its first incision at heterogeneous sites within a ∼500-nucleotide interval from the 3′ end of the DSB (20).

Here, we extend these foundational studies of AdnAB in two directions: biochemical and genetic. We address biochemically the effects of ATP availability on the rate and extent of unwinding of DSB ends, and visualize an end-bound AdnAB initiation complex and unwinding intermediates by atomic force microscopy (AFM), and describe the ability

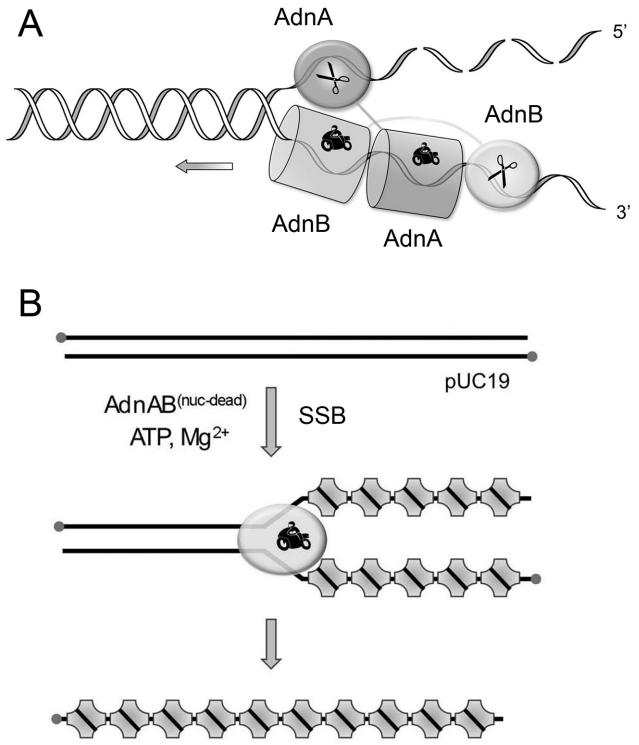

Figure 1. Division of labor during AdnAB dsDNA unwinding, processing of DSB ends, and capture of the unwound DNA strands by SSB. (**A**) Binding of AdnAB to the DSB end initiates ATP-dependent translocation of the tandem motor in the 3′ to 5′ direction along one of the DNA strands, with the dominant AdnB motor domain in the vanguard. Unwinding of the DNA duplex by the AdnB motor results in pumping of the 3′ ssDNA strand through the AdnA motor domain and into the AdnB nuclease domain and in threading of the 5′ ssDNA strand through the AdnA nuclease domain. (**B**) SSB tetramers bind to the single-stranded DNA formed in the wake of the AdnAB motor to yield SSB–ssDNA complexes, initially as Y-forked intermediates ultimately as fully unwound SSB–ssDNA end-products.

of the AdnA nuclease to 'nibble' the 5′ DSB end in the absence of ATP (implying that initial binding of AdnAB elicits melting of the dsDNA end). Genetically, we aimed to clarify which activities of AdnAB—ATPase, nuclease, or both, and of which subunit—are relevant to its role in HR and DNA damage repair *in vivo*, by inactivating each of the four catalytic domains of the AdnAB heterodimer, individually and in various combinations. The surprising and instructive findings were that a complete nuclease-dead AdnAB enzyme can sustain recombination (even more effectively than wild-type AdnAB in the I-Sce1 chromosomal DSB repair assay), as long as its AdnB motor is intact and RecO and RecR are present. We conclude that AdnAB's processive DSB unwinding activity suffices for AdnAB function in HR. Although not excluding the existence of a backup nuclease, our findings raise the prospect that mycobacterial homology-directed repair can proceed via DSB unwinding and protein capture of the displaced 3′-OH single strand without a strict need for end-resection.

MATERIALS AND METHODS

Recombinant *M. smegmatis* AdnAB and SSB proteins

Wild-type AdnAB heterodimer and versions containing inactivating mutations in the nuclease or ATPase modules of one of both subunits were produced by co-expressing His_{10}Smt3-AdnA and AdnB in *E. coli* and then purified from soluble extracts by Ni-affinity chromatography, cleavage of the tag by Smt3-protease Ulp1, separation of native AdnAB from the His_{10}Smt3 tag by a second Ni-affinity step, followed by anion exchange chromatography and glycerol gradient sedimentation as described previously (12–14). *M. smegmatis* SSB was produced in *E. coli* as a C-terminal His-tagged fusion and purified from a soluble bacterial extract by sequential Ni-affinity, anion exchange, heparin agarose and gel filtration chromatography steps as described previously (13).

Atomic force microscopy

Samples (50 μl) were applied to a freshly cleaved mica plate. After 1 min, the mica plate was washed gently with water and dried in a stream of argon gas. The samples were imaged in air, at room temperature, under controlled humidity in tapping mode using a MFP-3D-BIO Atomic Force Microscope (Asylum Research, Goleta, CA, USA) equipped with an Olympus AC240TS-R3 (Asylum Research, Goleta, CA) silicon nitride probe ($k = \sim 1.7$ N/m).

M. smegmatis strains

To construct domain-specific point mutants of AdnAB in *M. smegmatis*, we used a method involving oligonucleotide-derived single-stranded DNA recombineering and mycobacteriophage-encoded proteins (21). We cloned the counter-selectable marker, *sacB*, in $pJV75_{amber}$ (21) at the NheI site to create pRGM18, which was then transformed into wild-type *M. smegmatis* to give rise to the strain Mgm1657. Briefly, 60-mer oligonucleotides encoding the mutations of interest in the *adnAB* locus were electroporated along with a *hyg*-reversion oligonucleotide into the strain Mgm1657 (subsequent to acetamide-induced expression of the phage protein Che9c gp61). Hygromycin-resistant colonies that arise by repair of the *hyg*-defective allele on pRGM18 plasmid were screened for acquisition of the desired *adnAB* mutation in the chromosome. To facilitate screening and detection, the mutations in different oligonucleotides were designed such that either a new restriction enzyme site was created or a previously existing one was lost upon mutation in the *adnAB* gene; screening was performed by PCR-amplifying the relevant segment of *adnAB* from the recovered hygromycin-resistant colonies and performing diagnostic restriction digestions of the PCR product. The presence of the targeted point mutation was confirmed by sequencing the *adnAB* gene segment. The bacteria were cured of the pRGM18 plasmid by sucrose counter-selection, to yield a clean AdnAB domain-specific point mutant that lacks any antibiotic resistance. To make double or triple *adnAB* mutants inactivated in two or three of the AdnAB domains, the same procedure was followed in a step-wise manner starting from a single point mutant. On average, we observed that the frequency of obtaining chromosomal point mutations by this method was 2–6%, which is in good agreement with the results of the Hatfull laboratory (21). To delete *recO* and *recR* in the *adnAB* double nuclease mutant, specialized transduction was used, as described earlier (11,22). These mutants were confirmed by Southern analysis for the *recO* or *recR* locus, and re-checked for the *adnAB* nuclease-inactivating mutations by genomic PCR and sequencing. *M. smegmatis* strains were grown at 37°C in LB medium supplemented with 0.5% glycerol, 0.5% dextrose and 0.1% Tween 80. When required for selection, 100 μg/ml hygromycin or 20 μg/ml kanamycin was included in the growth medium. A complete list of the *M. smegmatis* strains used in the study is provided in Supplementary Table S1 of the supplementary material, and the list of primers is included in Supplementary Table S2.

Ionizing radiation (IR) killing assay

IR sensitivity was gauged by using a ^{137}Cs source to irradiate log-phase cultures (A_{600} of 0.3–0.4) of the different *M. smegmatis* strains. Cells were collected by centrifugation and resuspended in PBS with 0.05% Tween 80. Aliquots (200 μl) of the resuspended cells were irradiated using a rotating platform to ensure equal exposure to each sample. Following IR exposure, serial 10-fold dilutions were plated, and surviving colonies were counted after 3 days. Percent survival was calculated after normalization to the colony counts obtained from the unexposed control cells. Each IR assay was performed twice with each experiment containing biologic duplicates, and the mean value of percent survival (with standard errors of the means [SEM]) for every strain is plotted in the figures shown. Mean survival differences between strains were compared using the unpaired Student's *t*-test, the *P* values were calculated, and $P < 0.05$ was considered as the threshold for significance.

I-SceI mediated chromosomal recombination assay

Repair of chromosomal DSBs inflicted by I-SceI was assayed as described previously (2). *M. smegmatis* wild-type

and mutant strains harboring the chromosomally integrated *lacZ* reporter construct, pRGM10, were transformed with the same molar amount of the I-SceI plasmid and the control vector plasmid to determine the frequencies of HR and SSA repair in these strains. For each strain, the experiment was performed at least thrice using different batches of competent cells, and results are expressed as mean values. Percent survival in this chromosomal DSB repair assay for each strain was calculated as the percentage of the number of transformants obtained with the I-SceI plasmid versus the transformants obtained with the vector plasmid. Percent survival values from three independent experiments using different batches of competent cells for the same strain were determined and the average value with SEM is presented. The HR and SSA events were distinguished among the blue colonies by scoring for kanamycin resistance, whereby the kanamycin-resistant colonies represent HR and kanamycin-sensitive colonies denote SSA. To ascertain the NHEJ events among white colonies, genomic PCR amplication using primers that flank the region containing two I-SceI sites in the *lacZ* reporter were carried out and colonies that revealed a deletion in this locus were indicative of NHEJ repair (2). Relative repair frequencies were compared between different strains using the formulae: Relative HR frequency = (HR events/total blue events) × (% blue); Relative SSA frequency = (SSA events/total blue events) × (% blue); Relative NHEJ frequency = (NHEJ events/total white events) × (% white). When differences in % survival were noted for different strains, the frequencies of the two homology-dependent repair outcomes (HR and SSA) were compared by calculating the absolute repair frequency, where the distribution of a particular kind of repair in the surviving cells is corrected for the observed survival for each strain. To calculate the absolute HR frequency, the following formula was used: (% survival) x (HR events/total blue events) x (fraction blue). To calculate the absolute SSA frequency, the following formula was used: (% survival) × (SSA events/total blue events) × (fraction blue).

RESULTS

Effect of ATP concentration on dsDNA unwinding by the AdnAB motor

Purified AdnA(D934A)–AdnB(D1014A) heterodimer, bearing nuclease-inactivating mutations in both subunits, was incubated with linear pUC19 DNA (digested with BamHI and 5′ ^{32}P-labeled at both DSB ends) in the presence of 2 mM magnesium, 5.8 μM purified SSB, and 25, 50, 100 or 1000 μM ATP. The reactions were quenched after 10, 20, 30 or 60 s with EDTA and the products were resolved by native agarose PAGE and visualized by autoradiography. After a 20 s reaction at 1 mM ATP, most of the input dsDNA was converted to fully unwound SSB–ssDNA complexes that migrated more slowly than free dsDNA (Figure 2). The unwound SSB–ssDNA complexes were evident at 10 s, along with Y-forked intermediates comprising duplex DNA with short or long SSB-coated displaced single-strands, as depicted in Figure 1A and B. Thus, the AdnAB motor can unwind duplex 2.7-kb pUC19 DNA in 1 mM ATP at a rate of ∼270 bp s^{-1}. Lowering the ATP concentration altered the kinetics of unwinding and the distribution of the partially unwound intermediates in an instructive fashion. At 100 μM ATP, it took 30 s to accumulate substantial levels of the fully unwound SSB–ssDNA complexes, signifying a reduced unwinding rate (∼100 bp s^{-1}). At 10 s in 100 μM ATP, the Y-forked intermediates with short single-stands, migrating just above the dsDNA, were the predominant species, whereas at 20 s in 100 μM ATP, these were converted to more slowly migrating Y-forked molecules with long displaced single-strands (Figure 2). Reduction of ATP to 50 μM downshifted the motor, to the extent that no fully unwound DNA was formed in a 60 s reaction with AdnAB. Rather, virtually all of the input substrate was converted to Y-forked intermediates with short single-stands after 10 s in 50 μM ATP and these species declined progressively at 20, 30 and 60 s, concomitant with the accumulation of Y-forked molecules with long displaced single-strands. The AdnAB motor was retarded further at 25 μM ATP, such that all of the dsDNA was converted in 10 s to Y-forks with short single-stands, the mobility of which shifted upward progressively at 20, 30 and 60 s (implying a slow increase in the size of the ssDNA tails), albeit with no conversion to the Y-forked molecules with long displaced single-strands during a 60 s reaction (Figure 2). These results indicate that ATP concentration governs the speed of DSB unwinding by the AdnAB motor, but not the initial engagement by AdnAB of the DSB end.

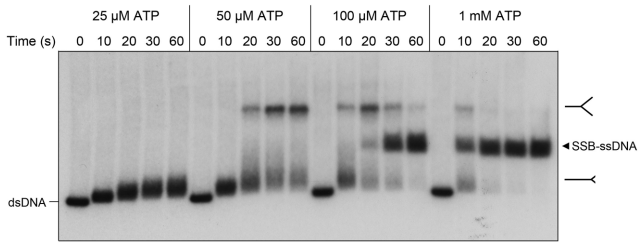

Figure 2. dsDNA unwinding by the AdnAB motor with strand capture by SSB. (**A**) Effect of ATP concentration on DSB unwinding. Reaction mixtures (50 μl) contained 20 mM Tris–HCl (pH 8.0), 1 mM DTT, 2 mM $MgCl_2$, 750 ng (427 fmol) of 5′ ^{32}P-labeled BamHI-cut pUC19 DNA, 700 ng (5.9 pmol) $AdnA^{D934}$•$AdnB^{D1014}$, and 575 pmol SSB. After withdrawing a time 0 sample (10 μl), the unwinding reactions were initiated by the addition of 25, 50, 100 or 1000 μM ATP. Aliquots (10 μl) were withdrawn after incubation at 37°C for 10, 20, 30 and 60 s and the reactions were quenched immediately by mixing with 10 μl of 50 mM EDTA, 15% glycerol, 0.125% Orange-G dye. The reaction products were analyzed by electrophoresis through a 0.8% native agarose gel in 40 mM Tris-acetate, 1 mM EDTA. The gel was dried under vacuum on DE81 paper. Radiolabeled DNAs were visualized by autoradiography.

Visualization of AdnAB unwinding intermediates by atomic force microscopy

To directly visualize AdnAB on DNA, we performed atomic force microscopy (AFM). AFM imaging of the products of the reaction of 'nuclease-dead' AdnAB with BamHI-cut pUC19 DNA in the presence of magnesium, but without ATP, revealed a predominance of linear dsDNA molecules with an AdnAB protein positioned at one of the DSB ends, and a minority of DNAs with proteins at both DSB ends (Figure 3A). The linear plasmids were not decorated at

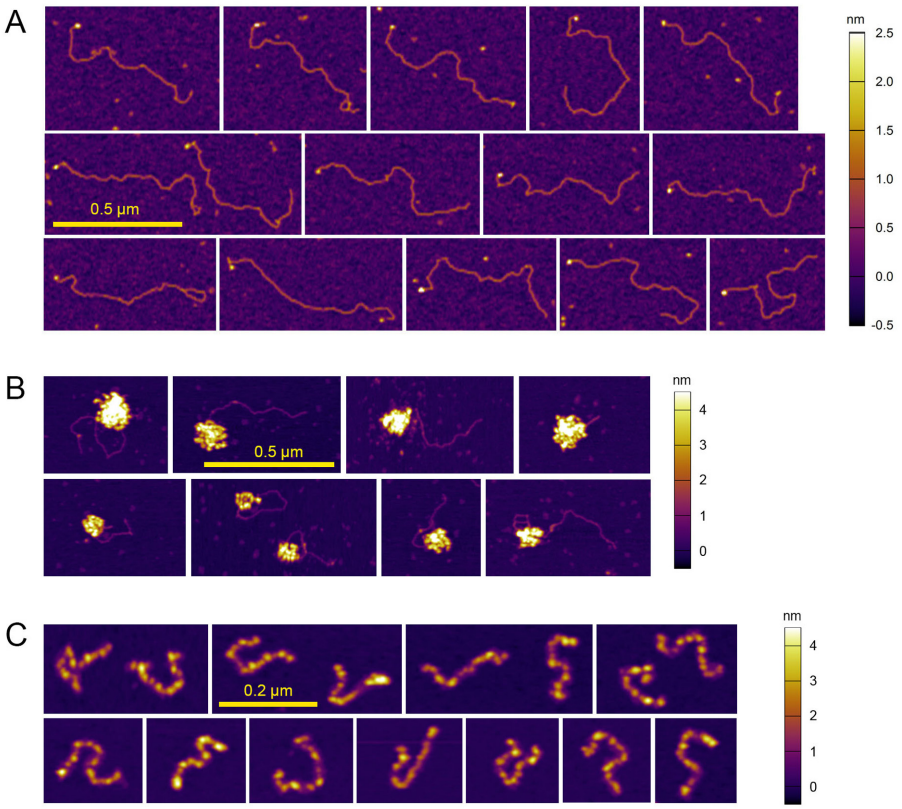

Figure 3. Visualization of unwinding reaction intermediates by atomic force microscopy. (**A**) A reaction mixture (10 μl) containing 20 mM Tris–HCl (pH 8.0), 2 mM $MgCl_2$, 150 ng (128 fmol) BamHI-cut pUC19, and 70 ng (0.6 pmol) $AdnA^{D934}AdnB^{D1014}$ (A^-B^-) were incubated for 30 s at 37°C. Reactions were quenched by adding 10 μl of 100 mM EDTA and placed on ice. For AFM, the samples were diluted 1:10 in 20 mM Hepes (pH 6.8), 5 mM $MgCl_2$. Aliquots (50 μl) were plated onto a freshly cleaved mica plate. AFM was performed as described in Methods. Images of individual linear dsDNAs with bright AdnAB 'dots' at one or both DSB ends are shown. (**B**) A reaction mixture (10 μl) containing 20 mM Tris–HCl (pH 8.0), 2 mM $MgCl_2$, 50 μM ATP, 150 ng (128 fmol) BamHI-cut pUC19, 70 ng (0.6 pmol) $AdnA^{D934}AdnB^{D1014}$ (A^-B^-), and 23 μM SSB were incubated for 30 s at 37°C. The reactions were initiated by adding ATP and quenched by adding 10 μl 100 mM EDTA. AFM images of lollipop-like unwinding intermediates are shown. (**C**) A reaction mixture (10 μl) containing 20 mM Tris–HCl (pH 8.0), 2 mM $MgCl_2$, 50 μM ATP, and 150 ng (128.2 fmol) BamHI-cut pUC19 was heated for 5 min at 95°C, then placed immediately on ice. The mixture was adjusted to 10 mM EDTA and supplemented with 23 μM SSB. AFM images of SSB–ssDNA complexes are shown. The color scales for height above the surface (in nm) from dark to bright are indicated on the right.

their ends when AdnAB was omitted from the reaction mixture (not shown). We surmise that the AdnAB motor forms a stable initiation complex at a DSB end that is then posed to unwind when provided with ATP (and SSB). Figure 3B shows AFM images of unwinding intermediates formed after a 30 s reaction of nuclease-dead AdnAB with pUC19 DNA in the presence of magnesium, limiting ATP (50 μM) and SSB. These were 'lollipop'-like structures consisting of a segment of duplex DNA at one end to which was attached a globular aggregate consisting of SSB-coated unwound ssDNA. The lengths of the dsDNA segment of the lollipops were variable, consistent with heterogeneity in the extent of unwinding by AdnAB during the 30 s reaction in 50 μM ATP (as also suggested by the data in Figure 2). These lollipop structures are virtually identical in appearance to lollipop-like structures visualized by AFM for *Bacillus* AddAB when it was reacted with linear plasmid DNA in the presence of ATP and *Bacillus* SSB (23). The globular appearance of the SSB-bound portion of the AdnAB-generated lollipop was distinct from that of the two-ended inchworm-like morphology of ssDNA–SSB complexes formed by reacting SSB with BamHI-cut pUC19 DNA that had been heated-denatured and quick-cooled on ice (Figure 3C). It is conceivable that the ssDNA is looped out from the advancing AdnAB motor, such that the ssDNA ends remains associated with AdnAB and do not extend to form a Y-shaped filament.

ATP-independent 'nibbling' of a 5′ DSB end by the AdnA nuclease

Prior studies employing short dsDNAs (12) and the present experiments with linear plasmid DNA (Figures 2A and 3A) indicate that: (i) AdnAB can bind stably to a DSB end in the absence of ATP; and (ii) ATP concentration does not significantly affect end capture. Studies of the *E. coli* RecBCD and RecBC enzymes have shown that their binding to a blunt DSB end in the absence of ATP elicits unpairing of the terminal 4–6 bp to form an 'initiation complex' for DNA unwinding (24,25). Were AdnAB to melt out a short segment of DNA at a DSB ends in an analogous ATP-independent manner, we would envision—in light of the division of labor among domains depicted in Figure 1A and our studies of AdnA nuclease action on ssDNA substrates (12)—that

melting might permit access of the 5′ strand terminus to the AdnA nuclease active site. To test this idea, we reacted wild-type AdnAB (nuclease active) with blunt end pUC19 DNA (linearized with SmaI and 5′ ^{32}P-labeled) or 5′-overhang pUC19 DNA (linearized with BamHI and 5′ ^{32}P-labeled) in the presence of magnesium but in the absence of ATP. The reactions were quenched with EDTA after 5 s, and 3, 10 or 20 min and the ^{32}P-labeled oligonucleotide products were resolved by denaturing urea-PAGE (Figure 4A). The reaction of AdnAB with the BamHI substrate resulted in the liberation of 5′ ^{32}P-labeled dinucleotide and trinucleotide cleavage products, detectable within 5 s, at which point 4.2% of the plasmid 5′ ends were cleaved, and increasing to 36%, 52% and 59% after 3, 10 and 20 min. The 5′ cleavages were suppressed completely by omission of magnesium (Figure 4A). AdnAB's reaction with the blunt-end SmaI substrate elicited release of 5′ ^{32}P-labeled dinucleotide and trinucleotide fragments, evident at 3 min (5.5% cleavage) and increasing at 10 (12% cleavage) and 20 min (15% cleavage) (Figure 4A).

To ascertain the source of the 5′ end-nibbling activity, we compared the reactivity of the BamHI substrate with wild-type AdnAB and variants with inactivation mutations in the AdnA nuclease active site (D934A; designated A^-B^+), the AdnB nuclease active site (D1014A; A^+B^-), or both nuclease active sites (A^-B^-). Whereas the AdnB nuclease mutation had no effect on 5′ nibbling, the AdnA nuclease mutation abolished nibbling (Figure 4B). Given that nibbling occurs on either a 5′ overhang or 5′ blunt DSB end, we conclude that AdnAB forms an initiation complex in the absence of ATP in which the strands undergo limited separation and the 5′ end is positioned in or near the AdnA nuclease active site.

In vivo domain-specific inactivation of *M. smegmatis* AdnAB

Although deletion of the *M. smegmatis adnAB* operon results in clastogen sensitivity and a two-fold-decrement in HR *in vivo* (2), it is not clear whether these effects are caused by absence of AdnAB protein (e.g. as a component of a larger repair machine) or the lack of one or more of AdnAB's catalytic functions. To investigate this issue, we employed an oligonucleotide-recombineering approach to allelic replacement (21) in order to introduce alanine mutations at the chromosomal *adnAB* locus (Figure 5A) that disable the AdnB ATPase (*adnB-D285A*), AdnB nuclease (*adnB-D1014A*), AdnA ATPase (*adnA-D255A*) or AdnA nuclease (*adnA-D934A*) activities (12,13). Oligonucleotides encoding these missense mutations were electroporated into wild-type *M. smegmatis* cells harboring the mycobacteriophage DNA recombineering machinery (see details in Materials and Methods). The desired mutants were identified by PCR amplification of the relevant *adnAB* segments from genomic DNA, diagnostic testing for intended loss or gain of a restriction site, and confirmation by sequencing the PCR product. For example, Supplementary Figure S1A (left panel) shows that a 740-bp PCR-amplified fragment spanning the *adnA* Asp255 codon generated two fragments of 403-bp and 337-bp upon treatment with SalI. However, the corresponding PCR-product from an *adnA-D255A* (motor-dead) mutant strain lacked the SalI site by design.

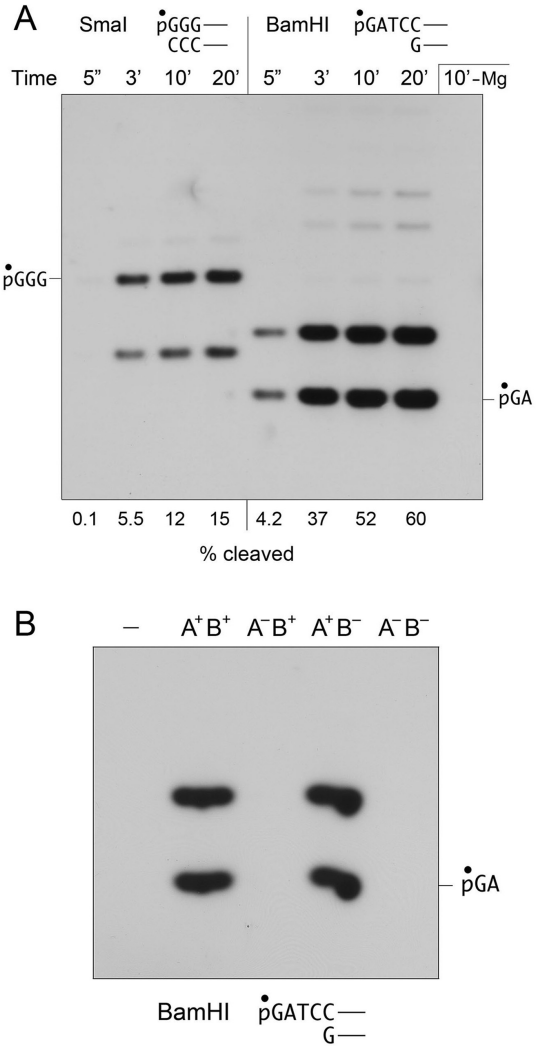

Figure 4. ATP-independent 'nibbling' of 5′ DSB ends by the AdnA nuclease. (**A**) Reaction mixtures (50 μl) containing 20 mM Tris–HCl (pH 8.0), 1 mM DTT, 2 mM $MgCl_2$, 2 mM ATP, 500 ng (285 fmol) 5′ ^{32}P-labeled SmaI-cut or BamHI-cut pUC19 (with 5′ termini as shown), and 400 ng (3.38 pmol) of wild-type AdnAB heterodimer were incubated at 37°C. Aliquots (10 μl) were withdrawn at the 5 s, 3 min, 10 min and 20 min (as specified above the lanes) and quenched by adding 10 μl of 90% formamide, 50 mM EDTA. A 10-min reaction of AdnAB with 5′ ^{32}P-labeled BamHI-cut pUC19 in the absence of magnesium is shown in the rightmost lane. The samples were heated for 5 min at 100°C and the reaction products were analyzed by electrophoresis through a 40-cm 24% polyacrylamide gel containing 7 M urea, 45 mM Tris-borate, 1.25 mM EDTA. An autoradiograph of the segment of the gel showing the 5′ ^{32}P-labeled oligonucleotides released by 5′ end nibbling is shown. The residual uncleaved pUC19 DNA was trapped at the top of the gel and is not shown. The extents of oligonucleotide release (as % of total radiolabeled DNA) were determined by scanning the gel with a Fujix imager and are shown at *bottom*. The identities of the cleavage products were determined by comparison to the oligonucleotides produced by secondary digestion of 5′ ^{32}P-labeled SmaI-cut pUC19 with BamHI (to generate 5′-pGGG) or 5′ ^{32}P-labeled BamHI-cut pUC19 with DpnI (to release 5′-pGA). The positions of the pGGG and pGA markers are indicated at left and right. (**B**) Reaction mixtures (10 μl) containing 20 mM Tris–HCl (pH 8.0), 1 mM DTT, 2 mM $MgCl_2$, 2 mM ATP, 100 ng (85.5 fmol) 5′ ^{32}P-labeled BamHI-cut pUC19, and 80 ng (0.68 pmol) wild-type AdnAB wild type (A^+B^+), $AdnA^{D934}$•AdnB (A^-B^+), AdnA•$AdnB^{D1014}$ (A^+B^-), or $AdnA^{D934}$•$AdnB^{D1014}$ (A^-B^-) were incubated for 3 min at 37°C. The reactions were quenched with formamide, EDTA and analyzed as described in panel A. AdnAB was omitted from the control reaction in lane –.

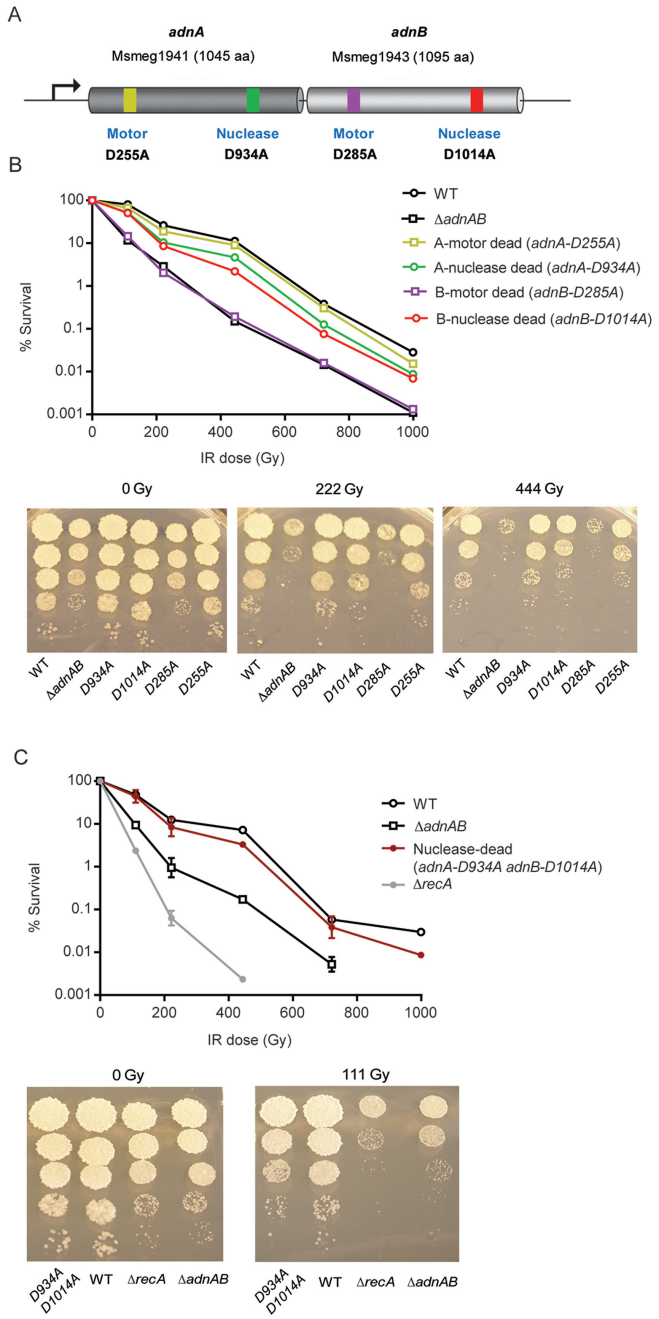

Figure 5. Clastogen sensitivity of AdnAB helicase and nuclease deficient *M. smegmatis*. (**A**) Domain organization of the *M. smegmatis* AdnAB heterodimer showing the helicase (motor) and nuclease active site residues targeted for mutation. (**B**) Survival curves of WT *M. smegmatis*, Δ*adnAB*, *adnA D255A*, *adnA D934A*, *adnB D285A* and *adnB D1014A* strains exposed to the escalating doses of ionizing radiation indicated on the *x* axis. Survival is plotted on a log scale (y axis) and is calculated compared to an unexposed control for each strain. (**C**) Survival curves of WT *M. smegmatis,* nuclease-dead (*adnA-D934A adnB-D1014A*), Δ*adnAB*, and Δ*recA* strains. Below the graph in both panels, representative 10-fold dilutions of the indicated strains, either untreated or IR treated (222 Gy and 444 Gy in panel A; 111 Gy in panel C), are shown. For each panel, percent survival for every strain was determined by culturing serial dilutions on agar plates after exposure to the indicated dose of IR. Each graphed point represents the mean from biological duplicates, and error bars are SEM; when they are not visible, they are within the symbol. In panel C, no viable counts were obtained for the Δ*recR* and Δ*adnAB* strains at the highest dose of IR exposure. Because 0% survival cannot be plotted on the logarithmic *y*-axis, these data points are not visible.

In the same way, the nuclease-dead *adnA-D934A* mutant strain was identified via a 803-bp PCR product, which was cleaved by SalI when amplified from wild-type *M. smegmatis* (to give 580-bp and 223-bp fragments) but resistant to SalI when amplified from the mutant strain (Supplementary Figure S1A, right panel). In case of *adnB*, incorporation of the *D285A* mutation conferred the gain of a NmeAIII restriction site within a 284-bp PCR product (yielding 178-bp and 106-bp fragments) that was not present in wild-type cells (Supplementary Figure S1B, left panel). The *adnB-D1014A* mutation resulted in a new BstNI restriction site within a 562-bp PCR fragment that generated 415-bp and 147-bp cleavage products. A double nuclease-dead *adnAB* strain was generated by introducing the *adnB-D1014A* mutation into *adnA-D934A* cells (Supplementary Figure S1C).

Effect of ATPase-dead and nuclease-dead AdnAB mutations on sensitivity to IR

We exposed mutants defective in each of the four catalytic domains of AdnAB to increasing doses of IR and compared their survival with that of wild-type and Δ*adnAB* strains. The Δ*adnAB* strain was 76-fold more sensitive to killing by 444Gy IR than wild-type *M. smegmatis* (Figure 5B). The *adnA-D255A* strain (AdnA motor-dead) resembled the wild-type with respect to IR sensitivity. In contrast, the *adnB-D285A* mutant (AdnB motor-dead) was hypersensitive to IR and phenocopied the Δ*adnAB* strain (Figure 5B), indicating that AdnB ATPase-helicase is necessary for AdnAB function in the repair of IR damage. The *adnB-D285A* mutant also shares a slow-growth phenotype with the Δ*adnAB* mutant in the absence of any exogenous DNA damage, as signified by their small colony sizes compared to WT and other *adnAB* mutants shown in the untreated controls of Figure 5B. These results collectively highlight that the AdnB motor is critical for AdnAB function *in vivo*.

Inactivation of either of the nuclease domains conferred slight sensitivity to increasing IR doses *vis à vis* wild-type (3-fold in the case of *adnA-D934A*; 5-fold for *adnB-D1014A,* at the dose of 722 Gy). These results raised the prospect that the AdnA and AdnB nucleases might be functionally redundant for IR damage repair. Thus, we constructed and tested a double nuclease-dead *adnA-D934A adnB-D1014A* strain, which, to our surprise, was hardly more sensitive to IR than the wild-type strain (1.5-fold at the dose of 722 Gy, with $P = 0.768$) and was clearly not as IR-sensitive as Δ*adnAB* or Δ*recA* (Figure 5C). Based on these results, we conclude that nuclease activity of AdnAB is largely dispensable for AdnAB function in IR damage repair.

Distinctive effects of AdnA and AdnB ATPase mutations on homologous recombination

To test the effect of AdnAB active site mutations on DSB repair *in vivo*, we employed the I-SceI-induced chromosomal DSB reporter system described previously (2,9,11). The reporter locus consists of two inactive *lacZ* alleles separated by a kanamycin-resistance marker (Figure 6A). The upstream *lacZ::I-SceI* allele is interrupted by two inverted I-SceI cleavage sites. The downstream *lacZ*-Δ*N* has no promoter and is missing the N-terminal coding sequence. The

A

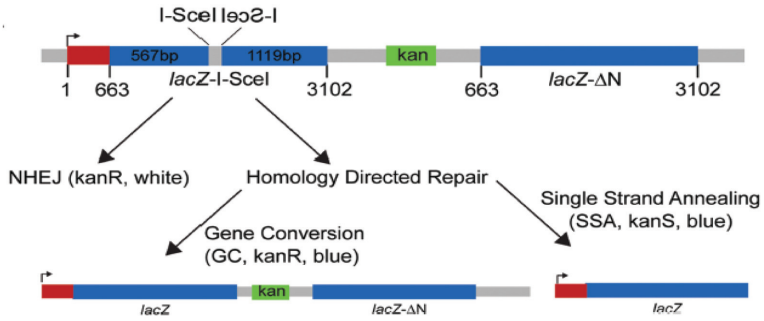

B

Strain	% Survival Mean (SEM)	% Blue Mean (SEM)	# blue	HR	SSA
WT	0.034 (0.001)	48.2 (0.9)	41	32	9
adnA-D255A (motor)	0.032 (0.002)	19.8 (0.50)	65	10	55
adnB-D285A (motor)	0.038 (0.001)	2.3 (0.20)	9	2	7
adnA-D934A (nuc)	0.031 (0.003)	9.3 (0.30)	32	23	9
adnB-D1014A (nuc)	0.033 (0.002)	30.9 (0.20)	56	49	7
adnA-D934A adnB-D1014A	0.97 (0.003)	74.9 (0.50)	150	148	2
Δ*adnAB*	0.036 (0.002)	29.33 (0.48)	44	36	8

C

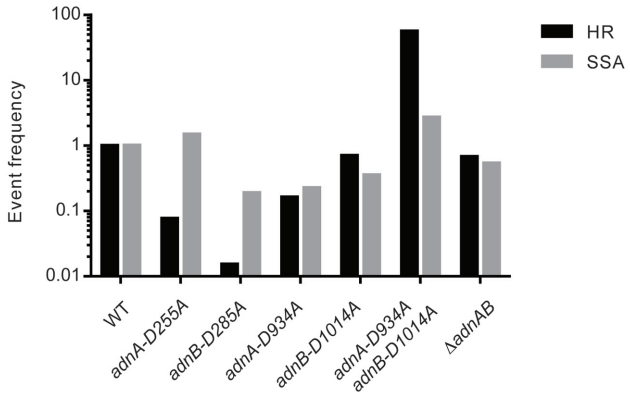

Figure 6. Role of AdnAB helicase and nuclease activities in DSB repair by recombination. (**A**) Schematic of the outcomes in the I-SceI-mediated DSB repair assay, adapted from (2). An I-SceI-induced DSB is initiated by transformation of a plasmid encoding I-SceI into a strain bearing a previously described (2, 9, 11) I-SceI recombination substrate. Repair of this DSB yields either blue or white colonies. White colonies can result either from NHEJ-mediated repair or inactivation of the I-SceI enzyme through mutation. Blue colonies indicate that the defective *lacZ* coding sequence has been restored either through single-strand annealing (SSA) or gene conversion/homologous recombination (GC/HR). DNA resection that occurs during SSA results in deletion of the kanamycin marker, whereas GC does not. (**B**) Percent survival, percent blue, and pathway outcome for each strain. # blue, the number of blue colonies genotyped to give the HR and SSA numbers. (**C**) Graph of HR and SSA event frequencies according to strain genotypes. The event frequency depicted is calculated as the absolute HR or SSA frequency for a particular strain normalized to that of WT *M. smegmatis.* For each strain, the absolute HR or SSA frequency is calculated from the genotyping algorithm shown in panel A, and the raw data are presented in the table in panel B. The absolute HR frequency is determined using the formula: (% survival) x (HR events/total blue events) x (fraction blue), and the absolute SSA frequency is calculated using the formula: (% survival) x (SSA events/total blue events) x (fraction blue).

reporter strain forms white colonies on X-gal medium. A unique chromosomal DSB is triggered by transforming the reporter strain with a hygromycin-resistance plasmid bearing I-SceI driven by a constitutive mycobacterial promoter. Survival on hygromycin in the face of I-SceI cleavage is contingent on repair of the DSB in a way that eliminates the I-SceI sites, either by unfaithful NHEJ (in which the survivors retain white colony color) or by homology-directed recombination—either HR or SSA—that results in blue colony color. As shown in Figure 6A, HR and SSA are readily distinguished by whether the blue survivors are kanamycin-resistant (HR) or kanamycin-sensitive (SSA).

In the wild-type cells, transformation with the I-SceI plasmid elicited massive lethality with a net survival of 0.034% (Figure 6B), as reported previously (2,9). The Δ*adnAB* mutant showed a similar survival of 0.036%, but there was a 2-fold decrement in HR (Figures 6B-C). The HR frequency in the *adnA-D255A* strain, in which the AdnA motor was mutated, was 12-fold lower than wild-type (Figure 6C). SSA was unaffected by the *adnA-D255A* mutation. A key finding was that HR frequency in the *adnB-D285A* strain with an inactive AdnB motor was 74-fold lower compared to wild-type, and 6-fold lower than the AdnA ATPase mutant. Most notable was that the decrement in HR in the *adnB-D285A* and *adnA-D255A* strains was much more severe (by 37-fold and 6-fold, respectively) than that in the Δ*adnAB* strain (Figure 6), indicating that the motor mutants are neomorphic and have a negative effect on HR. In the case of the AdnB motor-dead mutant, we suspect that stable binding of the helicase-dead AdnAB complex to DSB ends might inhibit the parallel pathway of AdnAB-independent HR that relies on RecO (9).

We observed previously that the HR and NHEJ pathways compete in the cell for DSB repair, whereby loss of NHEJ in Δ*ku* or Δ*ligD* strains is compensated by an increased frequency of HR events (2). A similar reciprocal relationship between homology-dependent and homology-independent repair mechanisms was observed in the AdnAB motor mutants. As compared to the wild-type strain, a concomitant increase in relative NHEJ frequency by 4.7-fold and 6.6-fold was noted in the *adnA-D255A* and *adnB-D285A* strains, respectively, as indicated by PCR analysis of the DSB locus in the white colonies, wherein we amplified the repair junctions from surviving white colonies, which represent a mixture of NHEJ-mediated repair events and unmodified sites due to inactivation of the I-SceI enzyme (2). Out of the 27 white colonies analyzed by PCR amplification and sequencing for either of the two motor-domain mutants (Supplementary Figure S2), 9 (in case of *adnA-D255A* mutant) and 6 (in case of *adnB-D285A* mutant) showed intact chromosomal loci with unmodified I-SceI sites (1350-bp amplification product with primer pair 1 or 2,167-bp amplification product with primer pair 2), whereas the remaining 18 and 21 events in the two respective mutants entailed deletions (<2 kb) with the characteristic NHEJ outcomes (bidirectional/unidirectional deletions and cross-break fill-in) previously observed in the wild-type strain (2). These results indicate that inactivation of the AdnAB ATPases, causing 12- to 74-fold decrements in HR, results in enhanced NHEJ. This effect on NHEJ was not evident in the complete absence of AdnAB protein, likely because HR was decreased by only 2-fold in the Δ*adnAB* strain (2). The present findings underscore that; (i) the mycobacterial NHEJ and HR repair systems are competitive with respect to their actions at a chromosomal DSB; and (ii) a helicase-inactive AdnAB complex does not block access of NHEJ factors to DNA, even though it inhibits alternative pathways of HR.

Role of AdnAB nuclease activities in HR

We next interrogated the effect of AdnAB nuclease mutations. Inactivation of the AdnA nuclease activity through the *adnA-D934A* mutation impaired HR by ∼5-fold (Figures 6B-C). By comparison, inactivation of the AdnB nuclease had little effect on HR (Figure 6C). In sharp contrast to our expectation that crippling the nuclease activity of the AdnAB complex would impair HR through abolition of end resection, we observed a dramatic enhancement of HR in the AdnAB double nuclease-dead strain, as measured by both relative and absolute HR frequencies after an I-SceI break. The enhanced HR of the AdnAB nuclease dead strain is the result of two effects; a 29-fold enhancement of survival and a 2-fold enhancement of the proportion of repair via the HR pathway (74% versus 38%), giving rise to a 60-fold higher absolute HR frequency than wild-type. These data clearly indicate that: (i) the nuclease activity of AdnAB is dispensable for mycobacterial HR; and (ii) the critical function supplied by AdnAB during DSB repair is its helicase activity, catalyzed by the motor in the AdnB subunit.

Homologous recombination in the absence of AdnAB nucleases requires the AdnB helicase and RecOR

The enhanced HR frequency and cell survival after an I-Sce1 induced DSB that was observed for the nuclease-dead *adnA-D934A adnB-D1014A* strain could either be due to an alternate pathway of HR that does not require AdnAB (9), or proceed through the AdnAB pathway, albeit without AdnAB-mediated resection. To address this issue, we introduced the AdnB motor-dead mutation *D285A* into the AdnAB double nuclease-dead strain and confirmed the genotype by diagnostic NmeAIII cleavage of a PCR-amplified 284-bp segment followed by sequencing (Supplementary Figure S3). When tested in the I-SceI system, HR was reduced by 60-fold in the *adnB-D285A adnA-D934A adnB-D1014A* triple mutant (Figure 7A, B) compared to the nuclease-dead *adnA-D934A adnB-D1014A* strain, signifying that the elevated recombination in the double nuclease-dead strain proceeds through DSB unwinding catalyzed by the AdnB motor of AdnAB. Similarly, the enhanced survival after I-SceI induction in the nuclease-dead *adnA-D934A adnB-D1014A* strain was reverted by inactivation of the AdnB motor (Figure 7A, B).

We next investigated whether the enhanced HR observed in the *adnA-D934A adnB-D1014A* strain requires the RecFOR system. We showed previously that all HR in mycobacteria requires RecR (11), whereas a subset of AdnAB-independent HR events requires RecO. We deleted either *recR* or *recO* in the AdnAB double nuclease-dead strain (Supplementary Figure S4) and assayed DSB repair via the

A

Strain	% Survival Mean (SEM)	% Blue Mean (SEM)	# blue	HR	SSA
WT	0.030 (0.002)	49.0 (0.4)	75	62	13
adnB D285A adnA D934A adnB D1014A	0.028 (0.001)	1.7 (0.1)	2	2	0
ΔrecO adnA D934A adnB D1014A	0.021 (0.003)	0.0 (0.0)	0	0	0
ΔrecR adnA D934A adnB D1014A	0.022 (0.002)	0.2 (0.2)	1	0	1
adnA D934A adnB D1014A	0.81 (0.002)	75.4 (0.2)	52	51	1

B

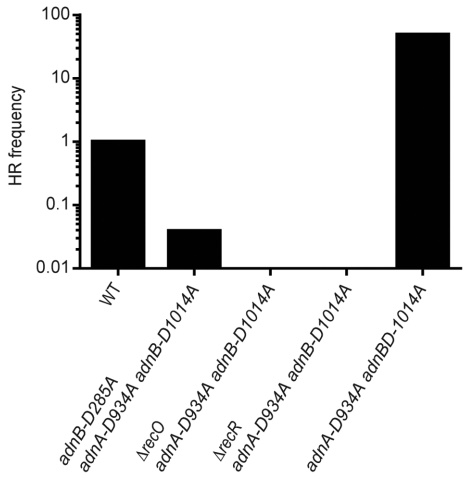

Figure 7. Role of AdnB helicase and RecFOR in AdnAB nuclease-independent HR. (**A**) Raw data of percent survival, percent blue and number of HR/SSA outcomes for indicated strains in the I-SceI assay. (**B**) Graphical representation of the HR event frequencies for the indicated strains. As in Figure 6C, event frequencies are calculated as the absolute HR frequency for a particular strain normalized to that of WT *M. smegmatis*.

I-SceI system (Figure 7). The key finding was that the enhanced HR of the AdnAB double nuclease-dead strain was abolished by deletion of *recR* or *recO* (Figure 7A and B). These data indicate that the enhanced HR present in the double nuclease dead strain requires the RecOR system, likely acting as RecA mediator. We interpret these results to indicate that in the absence of the AdnAB nucleases, recombination proceeds efficiently by using the same molecular machinery (i.e. AdnB motor, RecFOR, RecA) as wild type cells.

DISCUSSION

AdnAB is a vigorous ATP-dependent 3′ to 5′ DNA helicase and dsDNA exonuclease (12,14). Ensemble biochemical studies of AdnAB, and single-molecule visualization of AdnAB–DNA interaction by AFM, establish that AdnAB binds to DSB ends independent of ATP to form an initiation complex, apparently accompanied by localized fraying of the duplex at the DSB end that allows ingress of the 5′ DNA end to the active site of the AdnA nuclease. AdnAB then commences ATP-dependent DSB unwinding via processive translocation of the AdnB motor along the 3′ DNA strand. Unwinding feeds the 3′ strand through the AdnA motor, after which it is accessible to the AdnB nuclease. Whereas the AdnA and AdnB nucleases can incise the 5′ and 3′ displaced strands, respectively (Figure 1A) (10–12), it is unclear how the balance of 5′ versus 3′ strand cleavage is established to generate a stable 3′ tail serving as the substrate for RecA-mediated strand exchange. Initial decoration of the displaced DNA strands with SSB keeps them from reannealing behind the advancing AdnAB motor (Figure 1B) and also protects the displaced strands from a secondary round of degradation by AdnAB (11). Productive recombination would entail an exchange of RecA for SSB on the displaced 3′ strand. Because the contribution of the individual AdnAB enzymatic functions to recombination *in vivo* was unclear, we conducted a genetic analysis of the effects of ATPase-dead and nuclease-dead mutations, *per se* and in various combinations. The results prompt us to re-evaluate the presumption that extensive end-resection is an obligate step in bacterial homologous recombination.

AdnAB can drive recombination without its nuclease activities

The accepted model of recombination in bacteria and eukarya is that end resection is essential to generate the sub-

strate for recombinase loading. This model is based on the widespread participation of helicase–nuclease machines in recombination, the genetic dependence of the process on these helicase–nucleases, the direct demonstration (in budding yeast) of single strand resection at a DSB (26,27), and the biochemical properties of purified helicase–nuclease complexes. However, alternative models are possible, and have been proposed, in which recombinase loading could occur on the 3′ tailed strand of separated but unresected DNA (28). In this scheme, a helicase would be required to separate the strands, and SSB might be needed to keep the strands from reannealing, but then RecA loading would occur on the 3′ tailed strand.

Escherichia coli lacking the RecD subunit of RecBCD lacks the nuclease activity of RecBCD but is still recombination proficient. In this strain, the nuclease is supplied by RecJ or additional nucleases, indicating that resection is still required in this strain, but supplied by alternative nucleases (29–32). In an *E. coli* strain expressing the mutant RecB^{D1080A}CD enzyme, which is nuclease-dead and defective for the RecA loading function of RecBCD (33), homologous recombination is reduced 6-fold as measured by Hfr crosses; this effect is much milder than the 200-fold HR decrement seen in a Δ*recBCD* null strain (34). The residual chromosomal recombination in the *recB^{D1080A}CD* strain, but not in the wild type *recBCD* background, is abolished by mutation of *recO*, *recR*, or *recF* (34). Similarly, SOS induction requires the RecA-loading activity of RecO in the *recB^{D1080A}CD* background (35). The use of a similar 'hybrid' HR pathway has been reported for the *E. coli recB^{D1080A} recD* double mutant (which displays wild-type HR frequency in Hfr crosses; (34)), wherein the helicase activity is contributed by the mutant RecB^{D1080A}CD, but there is a requirement of RecJ for 5′ to 3′ exonuclease activity and a partial requirement of RecO for RecA loading function to support recombination (36). Thus, when the nuclease activity of *E. coli* RecBCD is lost, recombination is partially lost, but the residual recombination depends on the activity of nucleolytic and RecA loading functions from other pathways, which contribute little to recombination in RecBCD nuclease-proficient cells. Our results with nuclease-dead AdnAB differ from the findings in *E. coli* in that the vigorous recombination in the AdnAB nuclease-dead strain is not supported by a 'hybrid' backup pathway, but rather by the recombination factors required in wild type *M. smegmatis*, namely AdnB helicase, RecO and RecR.

To our knowledge, nuclease-deficient mutants of *B. subtilis* AddAB have not been examined *in vivo*. In *H. pylori*, either of the nucleases of the AddAB heterodimer is required for resistance to Ciprofloxacin, suggesting not only that resection is required for DSB repair, but also that there is no backup nuclease that can compensate (37). Thus, there is no evidence at present that recombination in bacteria that use AddAB enzymes can proceed through RecA loading on ssDNA generated solely by strand separation rather that strand separation and coupled single strand degradation.

Here, we show that in *M. smegmatis* cells that completely lack AdnAB nuclease activity, homologous recombination is preserved, indeed enhanced, compared to wild-type cells. The enhancement reflects the increased survival of *adnAB* nuclease-dead cells during I-SceI challenge and a higher preference (percentage-wise) for HR as the survival mechanism. The extremely low survival of wild-type cells is sensible in light of the nature of the DSB repair assay, insofar as: (i) I-Sce1 expression from the transformed plasmid elicits efficient cleavage of virtually all chromosomal *lacZ* reporter cassettes in the chromosome (including replicated sister chromatids); (ii) DSB resection past the *lacZ* gene (a distance of 1.2-kb to the left of the break) eliminates HR as a repair option; (iii) DSB end resection into the nearest flanking essential genes in the *M. smegmatis* chromosome (located 19.4 kb to the left and 8.1 kb to the right of the sites, respectively) is necessarily lethal, even if repaired by NHEJ and (iii) the rate of AdnAB's motor *in vitro* indicates that its nucleases could resect past the 'lethality limit' in <1 min and past the 'HR limit' in as little as 5 s. When AdnAB is absent, survival after I-SceI-induced DSBs remains low, possibly because RecBCD can then access the DSBs and rapidly resect the flanking DNA. However, when AdnAB is helicase-active but nuclease-dead, the single-strands unwound by the motor are largely intact, accessible to SSB and thus protected, and ultimately available as substrates for RecA-mediated HR. It is clear that this enhanced HR in the absence of AdnAB nuclease activity still proceeds through the AdnAB enzyme complex, because inactivation of the AdnB ATPase abolished HR in the double nuclease-dead strain.

One way to explain these findings is that an alternative mycobacterial nuclease can compensate for the loss of AdnAB nuclease in DSB end resection. In *E. coli*, the 5′-to-3′ DNA exonuclease RecJ can substitute for the RecBCD nuclease in certain mutant backgrounds (35,36). RecJ belongs to the DHH phosphodiesterase enzyme superfamily. The *M. smegmatis* proteome includes a DHH protein encoded by the MSMEG_2630 gene. However, deletion of MSMEG_2630 does not confer enhanced sensitivity to DNA clastogens compared to wild-type *M. smegmatis* (Gupta and Glickman, unpublished results) and the MSMEG_2630 protein has been characterized as an oligoribonuclease with 3′-5′ exonuclease activity (38), i.e, it is not RecJ-like. To our knowledge, there has been no characterization reported of a mycobacterial DNA single-strand 5′-3′ exonuclease enzyme.

An alternative model for the preservation of HR in the absence of an AdnAB nuclease is that recombination is proceeding without end resection, as alluded to above. In this model, the RecA nucleoprotein filament is formed on the unwound 3′ single strand, via agency of SSB and the mycobacterial RecFOR machinery, and thus primed for homology search and 3′ strand invasion. One can speculate that the unresected 5′ DNA strand might either remain coated with SSB, or be assembled with RecA. In either case, the unresected 5′ DNA strand could be available for annealing to the displaced strand of a D-loop formed by invasion of the DNA 3′ strand into a homologous duplex.

The phenotype of the double nuclease-dead AdnAB is distinct from either single nuclease-dead version anent its ∼30-fold improved survival after I-SceI challenge, suggesting that both of the displaced strands must be spared resection to ameliorate I-SceI toxicity. The importance of a balance between the two nucleases is reflected in the finding that the single AdnB nuclease-dead strain was like wild-

type with respect to HR, whereas the HR was reduced in the single AdnA nuclease-dead strain (to a greater degree than Δ*adnAB*; again, a neomorphic effect). The two nuclease modules of AdnAB act independently *in vitro* and mutating either one of them does not affect activity of the other. We speculate that in the AdnA nuclease-dead strain, as the AdnAB motor unwinds the DSB, the 3′ single strand is cleaved by the AdnB nuclease but the 5′ single strand is not processed. This would create asymmetry in the wake of the motor that biases recruitment of SSB, and ultimately RecA, to the 5′ DNA tail, a situation not optimally conducive to HR.

Possible role of the AdnA ATPase

It is uncertain whether the AdnAB machine has evolved a mechanism to modulate its nuclease activities in order to produce 3′ single strands for RecA assembly, as *E. coli* RecBCD and *Bacillus* AddAB do through the agency of a Chi sequence in the 3′ DNA single strand. Chi is recognized by the 'eroded' helicase-like domains of the RecC and AddB subunits, which correspond to the AdnA ATPase domain in AdnAB. Chi capture triggers cleavage of the 3′ strand downstream of Chi, after which Chi remains engaged *in situ* and the 3′ strand is immune from further cleavage as unwinding and translocation proceed. These events are thought to elicit a conformational change in the motor-nuclease complex resulting in extrusion of the unwound 3′ strand through a new exit channel as a single-strand DNA loop that provides the substrate for RecA loading (16–18).

A distinctive feature of AdnAB is the 'intactness' of the AdnA ATPase site, which is not essential for the helicase activity of the AdnAB complex, but which the present study shows plays a role in HR *in vivo*, manifest in the *adnA-D255A* strain as a 12-fold decrement in HR in the I-SceI assay. We speculate that it is possible that ATP binding and hydrolysis by AdnA is a switch that modulates the recombination-promoting activity of the AdnAB complex (e.g. by clamping down on the 3′ strand as it threads through the ATPase domain and then triggering its cleavage and 3′ end capture), akin to the switch elicited in *Bacillus* AddAB when Chi is sensed by the inactive ATPase domain. This idea is consistent with the postulated evolutionary relationships between the three clades of bacterial motor-nuclease machines, whereby AdnAB (2-subunits; 2-motors; 2-nucleases) is regarded as an ancestral precursor to AddAB (2-subunits; 1-motor; 2-nucleases) and RecBCD (3-subunits; 2-motors; 1-nuclease), with the added inference that AdnAB exemplifies a putative Chi-independent motor-nuclease and that the innovation of Chi recognition is linked to the de-activation of an AdnA-like 'lagging' ATPase situated in the enzyme complex between the 'leading' motor domain and its trailing nuclease domain.

SUPPLEMENTARY DATA

Supplementary Data are available at NAR Online.

ACKNOWLEDGEMENTS

We are grateful to AFM lab staff Matthew Brendel and Navid Paknejad for their assistance and guidance.

FUNDING

National Institutes of Health (NIH) [AI64693 to M.S.G., S.S.]; MSKCC AFM core lab is supported by NCI [P30 CA008748]. Funding for open access charge: NIH [AI64693].
Conflict of interest statement. None declared.

REFERENCES

1. Aniukwu,J., Glickman,M.S. and Shuman,S. (2008) The pathways and outcomes of mycobacterial NHEJ depend on the structure of the broken DNA ends. *Genes Dev.*, **22**, 512–527.
2. Gupta,R., Barkan,D., Redelman-Sidi,G., Shuman,S. and Glickman,M.S. (2011) Mycobacteria exploit three genetically distinct DNA double-strand break repair pathways. *Mol. Microbiol.*, **79**, 316–330.
3. Smith,G.R. (2012) How RecBCD enzyme and Chi promote DNA break repair and recombination: a molecular biologist's view. *Microbiol. Mol. Biol. Rev.*, **76**, 217–228.
4. Dillingham,M.S. and Kowalczykowski,S.C. (2008) RecBCD enzyme and the repair of double-stranded DNA breaks. *Microbiol. Mol. Biol. Rev.*, **72**, 642–671.
5. Wigley,D.B. (2013) Bacterial DNA repair: recent insights into the mechanism of RecBCD, AddAB and AdnAB. *Nat. Rev. Microbiol.*, **11**, 9–13.
6. Kushner,S.R. (1974) In vivo studies of temperature-sensitive recB and recC mutants. *J. Bacteriol.*, **120**, 1213–1218.
7. Kooistra,J., Haijema,B.J., Hesseling-Meinders,A. and Venema,G. (1997) A conserved helicase motif of the AddA subunit of the Bacillus subtilis ATP-dependent nuclease (AddAB) is essential for DNA repair and recombination. *Mol. Microbiol.*, **23**, 137–149.
8. Stephanou,N.C., Gao,F., Bongiorno,P., Ehrt,S., Schnappinger,D., Shuman,S. and Glickman,M.S. (2007) Mycobacterial nonhomologous end joining mediates mutagenic repair of chromosomal double-strand DNA breaks. *J. Bacteriol.*, **189**, 5237–5246.
9. Gupta,R., Ryzhikov,M., Koroleva,O., Unciuleac,M., Shuman,S., Korolev,S. and Glickman,M.S. (2013) A dual role for mycobacterial RecO in RecA-dependent homologous recombination and RecA-independent single-strand annealing. *Nucleic Acids Res.*, **41**, 2284–2295.
10. Verma,P. and Greenberg,R.A. (2016) Noncanonical views of homology-directed DNA repair. *Genes Dev.*, **30**, 1138–1154.
11. Gupta,R., Shuman,S. and Glickman,M.S. (2015) RecF and RecR play critical roles in the homologous recombination and single-strand annealing pathways of DNA repair in mycobacteria. *J. Bacteriol.*, doi:10.1128/JB.00290-15.
12. Sinha,K.M., Unciuleac,M.-C., Glickman,M.S. and Shuman,S. (2009) AdnAB: a new DSB-resecting motor-nuclease from mycobacteria. *Genes Dev.*, **23**, 1423–1437.
13. Unciuleac,M.C. and Shuman,S. (2010) Double strand break unwinding and resection by the mycobacterial helicase–nuclease AdnAB in the presence of single strand DNA-binding protein (SSB). *J. Biol. Chem.*, **285**, 34319–34329.
14. Unciuleac,M.C. and Shuman,S. (2010) Characterization of the mycobacterial AdnAB DNA motor provides insights into the evolution of bacterial motor-nuclease machines. *J. Biol. Chem.*, **285**, 2632–2641.
15. Saikrishnan,K., Yeeles,J.T., Gilhooly,N.S., Krajewski,W.W., Dillingham,M.S. and Wigley,D.B. (2012) Insights into Chi recognition from the structure of an AddAB-type helicase–nuclease complex. *EMBO J.*, **31**, 1568–1578.
16. Krajewski,W.W., Fu,X., Wilkinson,M., Cronin,N.B., Dillingham,M.S. and Wigley,D.B. (2014) Structural basis for translocation by AddAB helicase–nuclease and its arrest at χ sites. *Nature*, **508**, 416–419.
17. Wilkinson,M. and Wigley,D.B. (2014) Structural features of Chi recognition in AddAB with implications for RecBCD. *Cell Cycle*, **13**, 2812–2820.
18. Gilhooly,N.S., Carrasco,C., Gollnick,B., Wilkinson,M., Wigley,D.B., Moreno-Herrero,F. and Dillingham,M.S. (2016) Chi hotspots trigger a conformational change in the helicase-like domain of AddAB to

activate homologous recombination. *Nucleic Acids Res.*, **44**, 2727–2741.
19. Reddy,M.S., Guhan,N. and Muniyappa,K. (2001) Characterization of single-stranded DNA-binding proteins from Mycobacteria. The carboxyl-terminal of domain of SSB is essential for stable association with its cognate RecA protein. *J. Biol. Chem.*, **276**, 45959–45968.
20. Unciuleac,M.-C. and Shuman,S. (2010) Double strand break unwinding and resection by the mycobacterial helicase–nuclease AdnAB in the presence of single strand DNA-binding protein (SSB). *J. Biol. Chem.*, **285**, 34319–34329.
21. van Kessel,J.C. and Hatfull,G.F. (2008) Efficient point mutagenesis in mycobacteria using single-stranded DNA recombineering: characterization of antimycobacterial drug targets. *Mol. Microbiol.*, **67**, 1094–1107.
22. Bardarov,S., Bardarov,S. Jr, Pavelka,M.S. Jr, Sambandamurthy,V., Larsen,M., Tufariello,J., Chan,J., Hatfull,G. and Jacobs,W.R. Jr (2002) Specialized transduction: an efficient method for generating marked and unmarked targeted gene disruptions in Mycobacterium tuberculosis, M. bovis BCG and M. smegmatis. *Microbiology*, **148**, 3007–3017.
23. Yeeles,J.T.P., van Aelst,K., Dillingham,M.S. and Moreno-Herrero,F. (2011) Recombination hotspots and single-stranded DNA binding proteins couple DNA translocation to DNA unwinding by the AddAB helicase–nuclease. *Mol. Cell*, **42**, 806–816.
24. Farah,J.A. and Smith,G.R. (1997) The RecBCD enzyme initiation complex for DNA unwinding: enzyme positioning and DNA opening. *J. Mol. Biol.*, **272**, 699–715.
25. Wong,C.J. and Lohman,T.M. (2008) Kinetic control of Mg2+-dependent melting of duplex DNA ends by Escherichia coli RecBC. *J. Mol. Biol.*, **378**, 761–777.
26. Mimitou,E.P. and Symington,L.S. (2008) Sae2, Exo1 and Sgs1 collaborate in DNA double-strand break processing. *Nature*, **455**, 770–774.
27. Sugawara,N. and Haber,J.E. (2012) Monitoring DNA recombination initiated by HO endonuclease. *Methods Mol. Biol.*, **920**, 349–370.
28. Kowalczykowski,S.C., Dixon,D.A., Eggleston,A.K., Lauder,S.D. and Rehrauer,W.M. (1994) Biochemistry of homologous recombination in Escherichia coli. *Microbiol. Rev.*, **58**, 401–465.
29. Chaudhury,A.M. and Smith,G.R. (1984) A new class of Escherichia coli recBC mutants: implications for the role of RecBC enzyme in homologous recombination. *Proc. Natl. Acad. Sci. U.S.A.*, **81**, 7850–7854.
30. Dermić,D. (2006) Functions of multiple exonucleases are essential for cell viability, DNA repair and homologous recombination in recD mutants of Escherichia coli. *Genetics*, **172**, 2057–2069.
31. Lloyd,R.G., Porton,M.C. and Buckman,C. (1988) Effect of recF, recJ, recN, recO and ruv mutations on ultraviolet survival and genetic recombination in a recD strain of Escherichia coli K12. *Mol. Gen. Genet.*, **212**, 317–324.
32. Lovett,S.T., Luisi-DeLuca,C. and Kolodner,R.D. (1988) The genetic dependence of recombination in recD mutants of Escherichia coli. *Genetics*, **120**, 37–45.
33. Anderson,D.G., Churchill,J.J. and Kowalczykowski,S.C. (1999) A single mutation, RecB(D1080A,) eliminates RecA protein loading but not Chi recognition by RecBCD enzyme. *J. Biol. Chem.*, **274**, 27139–27144.
34. Ivancić-Baće,I., Peharec,P., Moslavac,S., Skrobot,N., Salaj-Smic,E. and Brcić-Kostić,K. (2003) RecFOR function is required for DNA repair and recombination in a RecA loading-deficient recB mutant of Escherichia coli. *Genetics*, **163**, 485–494.
35. Vlasić,I., Ivancić-Baće,I., Imesek,M., Mihaljević,B. and Brcić-Kostić,K. (2008) RecJ nuclease is required for SOS induction after introduction of a double-strand break in a RecA loading deficient recB mutant of Escherichia coli. *Biochimie*, **90**, 1347–1355.
36. Ivancic-Bace,I., Salaj-Smic,E. and Brcic-Kostic,K. (2005) Effects of recJ, recQ, and recFOR mutations on recombination in nuclease-deficient recB recD double mutants of Escherichia coli. *J. Bacteriol.*, **187**, 1350–1356.
37. Amundsen,S.K., Fero,J., Salama,N.R. and Smith,G.R. (2009) Dual nuclease and helicase activities of helicobacter pylori AddAB Are required for DNA repair, recombination, and mouse infectivity. *J. Biol. Chem.*, **284**, 16759–16766.
38. Srivastav,R., Kumar,D., Grover,A., Singh,A., Manjasetty,B.A., Sharma,R. and Taneja,B. (2014) Unique subunit packing in mycobacterial nanoRNase leads to alternate substrate recognitions in DHH phosphodiesterases. *Nucleic Acids Res.*, **42**, 7894–7910.